Optimization of Grinding Performance of Tumbling Ball Mill*

Guoming HU**, Hideyuki OTAKI***
and Keiichi WATANUKI***

Based on motion and impact analysis, a theoretical model is presented for optimization of grinding performance of a tumbling ball mill. The motion of ball media in the tumbling ball mill is analyzed. The impact parameters of the ball media caused by the falling motion are deduced. The impact and attrition grindabilities are studied. The grinding performance is expressed as the proportion of grindability of all collisions to that of the collisions of ball media in the arc of the shell at a theoretically suitable speed, and is calculated from the point of view of the separation layer. The mathematical model is established and program coding is implemented to optimize grinding performance for the tumbling ball mill. An example of design calculations is given which shows that the grinding performance under the optimized operation parameters is improved significantly.

Key Words: Operation Planning, Rotary Machinery, Optimum Design, Grinding, Impact, Motion, Tumbling Ball Mill

1. Introduction

Tumbling ball mills, as types of rotary machinery, are of significant industrial importance. Figure 1 shows the vertical section through a single-compartment tumbling ball mill. The mill is characterized by a shell, which contains grinding ball media and ore, rotating about a horizontal axis. The mill shell is supported at both ends by trunnion bearings. The inside of the shell is lined. Usually, cast iron ball media are used, and brittle materials as ores are considered. Figure 2 shows the cross section of the mill. The mill charge includes ball media and particles of ore, and is divided into three zones: the ascending zone (A), the falling zone (B) and the grinding zone (C). The ball media gain potential energy and then cataract into the grinding zone. The comminuting action takes place by impacts from media, by rolling-action encounters between the ball media and the particles, and by the trapping of particles between ball media during their elevation by the cylinder shell. As a part of operation planning, the selection of operation parameters has direct influence on the grinding efficiency and production capacity of the tumbling ball mill. Although a large number of theoretical and experimental research studies have been conducted on the design and calculation of tum-

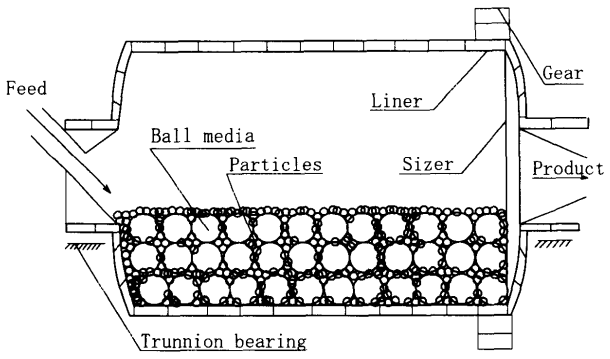

Fig. 1 Vertical section through a ball mill

* Received 11th May, 1999
** Doctoral Candidate, Course in Production Science, Graduate School of Science and Engineering, Saitama University, Japan. E-mail: sgd2936@post.saitama-u.ac.jp
*** Department of Mechanical Engineering, Faculty of Engineering, Saitama University, 255 Shimo-okubo, Urawa-shi 338-8570, Japan

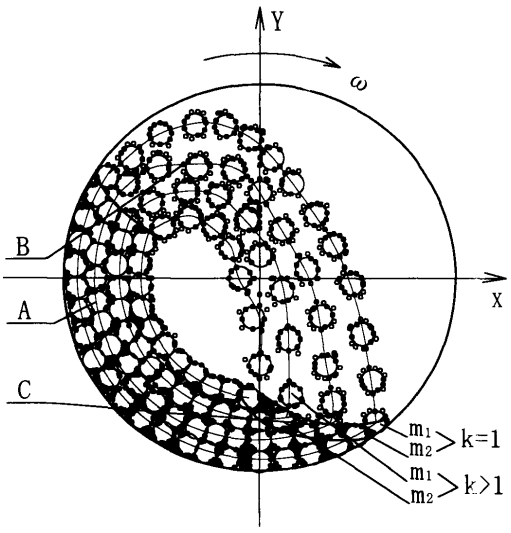

A	Ascending zone
B	Falling zone
C	Grinding zone
k	Number of layer

Fig. 2 Cross section of tumbling ball mill

bling ball mills, the main focus has been paid on the grinding technological process. The determination of operation parameters is mainly dependent on the theoretically suitable speed, the inner layer radius of the ball media and empirical knowledge. Bond[1] had proposed the selection of a grinding ball of suitable size for a high grinding efficiency. Viswanathan and Mani[2] had worked on the calculation of product distribution from a time-dependent distributed fracture model by the optimum method. Mishra and Rajamani[3],[4] performed a simulation of charge motion in ball mills by the discrete element method, which focused on ball segregation with rotary speed, frequency distribution of ball collision as a function of collision energy, and friction between the ball charge. Powell and Nurick[5]-[7] studied the nipping of the ore between balls, the dilation, migration and segregation of ball charge by X-ray films and r-camera filming techniques, and found that the face angle of lifter balls influences both the maximum impact energy and the amplitude of work done by the charge, and that the inner part of the cascading region and the toe region are responsible for the majority of the grinding work. These works provide useful information about mill design and optimization. In this paper, we establish a mathematical model for optimization of grinding performance for a tumbling ball mill based on the analysis of media motion and impact parameters, and obtain the optimal speed ratio, filling ratio and dimensions of the ball medium for various tumbling ball mills.

Nomenclature

A: radius of strain contact circle caused by impact force, m
A_e: maximum radius of strain contact circle caused by impact force, m
A_{ek}: maximum radius of strain contact circle of ball media at k layer, m
B: effect area nipped by ball media, m^3
B_k: effect area nipped by ball media at k layer, m^3
C_1, C_2: objective weighted factors
C_e: coefficient related to the surface energy of the material
E: Young's modulus of ball media, Pa
E_1, E_2: Young's moduli of collision balls, Pa
E_{imk}: energy related to impact grinding of ball media at k layer, J
E_{max}: allowable maximum energy of individual ball medium, J
F_1: area occupied by charge in ascending zone, m^2
F_2: area occupied by charge in falling zone, m^2
H: total falling height, m
J: number of cycles of tensile stress σ
K_{ic}: intensity factor of critical stress, $Pa \cdot m^{1/2}$
L: effective length of mill, m
M_1: total mass of charge, kg
M_m: total mass of ball media, kg
M_{1k}: mass of charge at k layer, kg
N: total numbers of layers of ball media
N_m: calculation power, kW
N_{motor}: power of the driving motor, kW
P: impact force produced by collision, N
P_e: maximum impact force produced by collision, N
P_{ek}: maximum impact force of ball media at k layer, N
R_k: radius of circle of ball media at k layer, m
R_ρ: radius of circle of leaving trajectory, m
V: relative velocity of collision balls, m/s
V_e: initial relative velocity of collision balls, m/s
W_1: impact grinding performance
W_2: attrition grinding performance
W_3: synthesized grinding performance
W_{imk}: impact grinding performance of ball media in k layer
W_{atk}: attrition grinding performance of ball media in k layer
a: length of the crack, m
e: impact force exponential
f_k: collision frequency of ball media at k layer, s^{-1}

g: acceleration due to gravity, m/s^2
h: elevated height of ball medium from leaving point, m
l: maximum radius of particle nipped by ball media, m
m: mass of single ball medium, kg
m_1, m_2: masses of collision balls, kg
n: yield exponential
r: radius of ball medium, m
r_1, r_2: radii of collision balls, m
r_{min}, r_{max}: minimum and maximum radii, respectively of ball medium, m
t_e: duration time of collision, s
t_{ek}: collision time of ball media at k layer, s
v_k: leaving speed of ball media at k layer, m/s
v_{ky}: y-coordinate section of v_k of ball media at k layer, m/s
v_{pk}: falling speed of ball media at k layer, m/s
v_{nk}: falling normal speed of ball media at k layer, m/s
v_{tk}: falling tangential speed of ball media at k layer, m/s
α_k: leaving angle of ball media at k layer, rad
λ_k: falling angle of ball media at k layer, rad
θ_k: $\pi/2-\alpha_k$, rad
β_k: $\pi-\lambda_k$, rad
δ: approaching distance of center of collision balls, m
δ_e: maximum approaching distance of center of collision balls, m
η_1: efficiency of transmission system
η_2: the overload coefficient of the motor
ψ: speed ratio of the running speed to the critical speed
ψ_{min}, ψ_{max}: minimum and maximum speed ratios, respectively
μ: Poisson's ratio of ball media
μ_1, μ_2: Poisson's ratio of collision balls
ν: coefficient of Coulomb friction
ϕ: filling ratio of ball media
ϕ_{min}, ϕ_{max}: minimum and maximum filling ratios, respectively of ball media
ϕ_g: filling ratio of ore
ε_g: porosity of ore
ε_m: porosity of ball media
ρ_g: density of ore, kg/m^3
ρ: density of ball media, kg/m^3
σ: tensile stress, Pa
ω: angular velocity of tumbling ball mill, rad/s

2. Motion and Impact Analysis of Ball Media

2.1 Motion analysis

In the bulk of the charge, away from the outer layer, the ideal layering charge is not likely to exist. Considering the natural packing of ball media, the layers will overlap each other[5]. A ball is (1) stacked on the top of another ball in the same layer; (2) stacked on the top of two balls in a concentric row, and (3) stacked between two layers, on the top of three ball media. So are the impacts between ball media. The outer layer of ball media being acted upon directly by the mill shell predominantly determines the motion of the entire charge; the motion of the charge in the ascending zone is simplified for each ball and each particle of the ore traveling on circular arcs, concentric with the mill shell, and there is no slip between the shell and the charge. As shown in Fig. 3, considering the ball media in a layer of radius R_k, the force equilibrium equation of the ball medium at the leaving point is expressed as $mR_k\omega^2=mg\cos\alpha_k$, the trajectory equations of the leaving points are given as follows:

$$X=R_k\sin\alpha_k \quad (1)$$

$$Y=R_k\cos\alpha_k \quad (2)$$

where

$$\alpha_k=\arccos(\omega^2R_k/g) \quad (3)$$

which means that the trajectory of the leaving points is an arc of the circle with the radius $R_\rho=g/(2\omega^2)$, and the center $(0, g/(2\omega^2))$ in the X-Y coordinate system. The speed of ball media at the leaving point is expressed by:

$$v_k=\sqrt{gR_k\cos\alpha_k} \quad (4)$$

After projecting from the leaving point, the ball medium follows a parabolic path. Its equation is $y=-x\tan\alpha_k+gx^2/(2v_k^2\cos^2\alpha_k)$. The dropping point of the ball medium is at the original layer of the circle of $X^2+Y^2=R_k^2$. As the relationship between the x-y coordinate and X-Y coordinate is $x=X+R_k\sin\alpha_k$ and $y=-Y+R_k\cos\alpha_k$, the trajectory equations of falling points are given by:

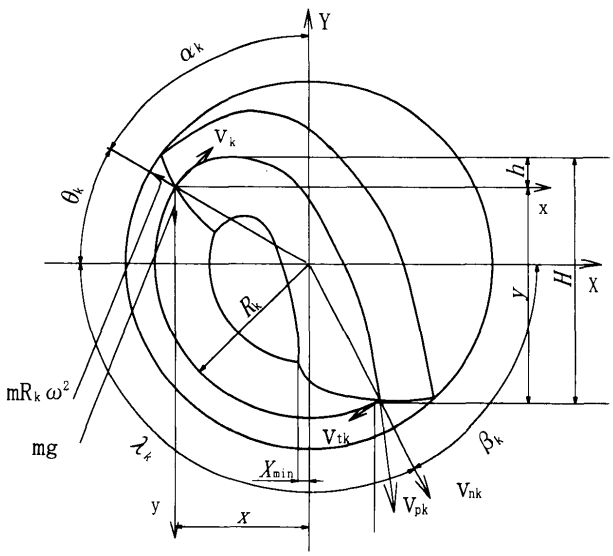

Fig. 3 Motion analysis of ball media

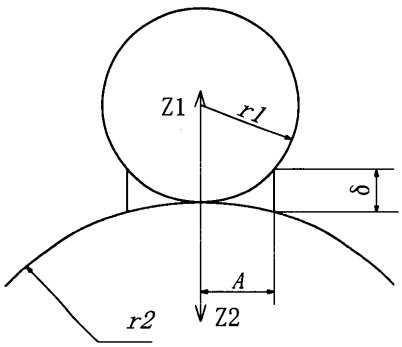

Fig. 4 Contact analysis of collision

$$x=4R_k \sin \alpha_k \cos^2 \alpha_k \quad (5)$$

$$y=4R_k \sin^2 \alpha_k \cos \alpha_k \quad (6)$$

As $\alpha_k=\pi/2-\theta_k$, rearranging Eq.(6) leads to $y=4R_k \cos^2 \theta_k \sin \theta_k$. From the geometric relationship in Fig. 3, y is also given by $R_k(\sin \theta_k+\sin \lambda_k)$. So the trajectory equation of falling points is also expressed as:

$$\lambda_k=3\theta_k \quad (7)$$

Next, the elevated height of the ball medium from the leaving point obtained according to parabola kinematics is $h=(v_k \sin \alpha)^2/(2g)$. The total falling height is $H=h+y$. Substituting h and Eq.(6) into H, yields $H=h+y=4.5R_k \sin \alpha_k \cos \alpha_k$. The horizontal speed v_x and vertical speed v_y are expressed as $v_k \cos \alpha_k$ and $\sqrt{2gH}$ respectively, and β_k equals $\pi-\lambda_k=3\alpha_k-\pi/2$, so the speeds of the ball media at dropping points are expressed as follows:

$$v_{pk}=\sqrt{v_x^2+v_y^2}=v_k\sqrt{9-8\cos \alpha_k} \quad (8)$$

$$v_{nk}=v_x \cos(3\alpha_k-\pi/2)+v_y \sin(3\alpha_k-\pi/2)$$
$$=8v_k \sin^3 \alpha_k \cos \alpha_k \quad (9)$$

$$v_{tk}=-v_x \sin(3\alpha_k-\pi/2)+v_y \cos(3\alpha_k-\pi/2)$$
$$=v_k+4v_k \sin^2 \alpha_k \cos(2\alpha_k) \quad (10)$$

2.2 Analysis of impact parameters

The impact force P varies with time t during collision. As shown in Fig. 4, if the approaching distance of the center of collision balls is δ, the relative normal velocity of two collision balls is V, and the impact force is P, then:

$$Pm_r=-dV/dt=-d^2\delta/dt^2 \quad (11)$$

where $m_r=1/m_1+1/m_2$. Hertz's theory predicts that:

$$P=(4/3)r_r^{-1/2}E_r^{-1}\delta^{3/2} \quad (12)$$

$$A=(3/4)^{1/3}r_r^{-1/3}E_r^{1/3}P^{1/3} \quad (13)$$

where $r_r=1/r_1+1/r_2$, and $E_r=(1-\mu_1^2)/E_1+(1-\mu_2^2)/E_2$. Substituting $d^2\delta/dt^2=VdV/d\delta$ and Eq.(12) into Eq.(11), we obtain:

$$VdV/d\delta=-(4/3)r_r^{-1/2}E_r^{-1}m_r^{-1}\delta^{3/2} \quad (14)$$

Integrating Eq.(14) with respect to V from 0 to its maximum value V_e, we obtain:

$$\delta_e=(5/3)^{2/5}r_r^{-1/5}E_r^{-2/5}m_r^{-2/5}V_e^{4/5} \quad (15)$$

Substituting Eq.(15) into Eqs.(12) and (13), we obtain:

$$P_e=(5/4)^{3/5}(4/3)^{2/5}r_r^{-1/5}E_r^{-2/5}m_r^{-3/5}V_e^{6/5} \quad (16)$$

$$A_e=(15/16)^{3/5}m_r^{-3/5}r_r^{-1/5}E_r^{3/5}V_e^{6/5} \quad (17)$$

In the same way, integrating Eq.(14) with respect to V from 0 to its arbitrary value V, the relationship between V and δ at any instance is given by $V=V_e\sqrt{1-(\delta/\delta_e)^{5/2}}$, which means:

$$d\delta/\sqrt{1-(\delta/\delta_e)^{5/2}}=V_e dt \quad (18)$$

Integrating Eq.(18) with respect to δ from 0 to its maximum value δ_e, we obtain the duration time of collision by:

$$t_e=2\delta_e/V_e\int_0^1 dx/\sqrt{1-x^{5/2}}$$
$$=2.943\,28(15/16)^{2/5}m_r^{-2/5}r_r^{-1/5}E_r^{2/5}V_e^{-1/5} \quad (19)$$

3. Grinding Performance Optimization of Tumbling Ball Mill

3.1 Grinding performance

Usually, the energy exerted on the ore bed is considered as the grindability, which correlates the energy with the mass and the speed of the ball medium. But Eq.(16) reveals that the impact force P_e also depends on the sizes and the material characteristics of the collision bodies. Moreover, even if the energies exerted are the same, the grinding efficiencies are evidently different as the collisions are of different kinds. In the present study, we analyze the grindability from the aspects of impact grinding and attrition grinding, and define the grinding performance as a dimensionless parameter in terms of the proportion of grindability of all collisions to that of the collisions of ball media in the outer layer at theoretically suitable speed. The impact grinding effect is mainly used in producing particles of 10 - 100 μm fineness, especially in the case where fine particles are not required. The attrition grinding effect is mainly used in producing particles of 1 - 10 μm fineness, and is used in producing spherical particles.

3.1.1 Impact grinding Normal impact velocity v_{nk} produces impact grinding to the ore. When the impact collision occurs between the ball media or between the liner and the ball medium, the ore around the media produces a cushioning effect, otherwise the collision is invalid. However, the impact force exerted on the ore bed is difficult to obtain; the impact force on the media is commonly taken as a design criterion. On the other hand, the size and density of the ball medium are much greater than those of the particles, and hence it is reasonable to omit the collisions of the particles.

From the point of view of grinding energy exerted, the grindability per unit time depends on the impact speed and the collision frequency:

$$E_{imk}=mv_{nk}^2 f_k/2 \quad (20)$$

In the cases that the same energy is exerted, the

high frequency of impact can remedy inadequate impact velocity:

$$f_k=(1/v_{nk}^2) \tag{21}$$

If the exerted force does not exceed the strain limit, the ore would be compressed and elastic strain would be produced. When the external load is off, the ore would return to the original shape and not be ground. But from the point of view of fracture mechanics[8], in the above process, although the ore is not destroyed, a new surface cannot be created, as numerous cracks are produced and particularly, the original cracks are extended in the ore. Because the stress at the peak of the crack exceeds the pulling stress vertical to the crack, the ore might be ground when the same force is exerted later. The stress criteria of brittle destruction and yield destruction are given by[9]:

$$\sigma=K_{ic}/(C_e\sqrt{a}) \tag{22}$$

$$\sigma^n J=\sigma_0^n J_0=\text{Const.} \tag{23}$$

where: the subscript 0 indicates the base cycles. The tensile force σ is emphasized because the brittle particle is loaded predominantly by impact and very large compressive stresses are generated at the contact point, substantial tensile stresses are also induced within the particle. The existing micro-flows intensify the applied tensile stresses and the particle fails at the large flaws[10]. Equation (22) is mainly applied for the primary breakage of particles while Eq.(23) is applied for the secondary breakage of particles.

The ore grinding in the mill generally involves multi-collision, and the grinding action involves brittle destruction yielding final particles of sizes larger than 30 μm, or synthesized destruction of yield and brittleness yielding particles ranging in size from 10 μm to 30 μm[11]. It can be considered that the ability of impact grinding is a function of impact force and frequency as $P_{ek}^e f_k$. As the grindability of the ball media of an assumed radius in the outer layer at a theoretically suitable speed is given by $P_{e0}^e f_0$, the impact grinding performance is defined as:

$$W_{imk}=P_{ek}^e f_k/(P_{e0}^e f_0) \tag{24}$$

where the subscript 0 indicates that those parameters represent the ball media in the arc of the shell.

3.1.2 Attrition grinding The ability of attrition grinding depends on the tangential velocity v_{tk} and the force P_{ek} caused by the normal velocity v_{nk}. As stated by Brach[12], tangential impact can occur only when the mass center trails the contact point in the initial tangential motion, and tangential force existing during contact can only be developed in the presence of a normal force. For the media impact in the tumbling ball mill resembling collinear collision, tangential impact causes media whirling. The radius of the strain contact circle caused by impact force is expressed by Eq.(17). Assuming Coulomb friction is valid in this zone, because of the presence of v_{tk}, the energy exerted on the ore is given by $\nu P_{ek} v_{tk} t_{ek}$, so the attrition grindability is expressed as the product of $\nu P_{ek} v_{tk} t_{ek}$ and A_e^2. The effective area nipped by the ball media as shown in Fig. 5 is given by $B=2\pi l^2(r+l/3)$, the energy exerted on the ore is expressed as $mv_{tk}^2/2$, so the attrition grindability in that zone is expressed as the product of $mv_{tk}^2/2$ and B.

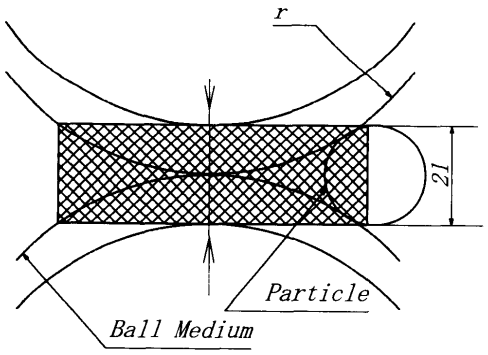

Fig. 5 The nipping zone between ball media

Comparing the attrition ability of all ball media to that of the ball media in the arc of the shell at a theoretically suitable speed yields the attrition grinding performance as:

$$W_{atk}=P_{ek}v_{tk}A_{ek}^2 f_k/(P_{e0}v_{t0}A_{e0}^2 f_0)+mv_{tk}^2 B_k f_k/(m_0 v_{t0}^2 B_0 f_0) \tag{25}$$

3.2 Mathematical model for performance optimization of tumbling ball mill

3.2.1 Objective function Considering the media-made motion in the separation layer, the ball media of the falling zone in the outer layer collide with the liner, and the ball media in other layers collide with other ball media. Hutching[13] and Thornton[14] discovered that when the impact velocity increased, the coefficient of restitution decreased accordingly. In the case of a tumbling ball mill, we can consider that due to the constraint by the shell and the surrounding media, the speed of the ball medium after the collision equals zero. Assuming that the radius and mass of the shell greatly exceed those of the medium, that is when $k=1$, then $m_2 \gg m_1=m$, and $r_2 \gg r_1=r$; and that the radius and mass of all media are equal, that is when $k>1$, then $m_2=m_1=m$ and $r_2=r_1=r$ (see Fig. 2), and the material characteristics of the media and the liner are the same, which means $E_1=E_2=E$ and $\mu_1=\mu_2=\mu$. From Eqs.(16), (17) and (19), we obtain the impact parameters as:

$$P_{ek}=\begin{cases}(5/4)^{3/5}(2/3)^{2/5}r^{1/5}m^{3/5}((1-\mu^2)/E)^{-2/5}V_e^{6/5} & k=1\\ (5/16)^{3/5}(4/3)^{2/5}r^{1/5}m^{3/5}((1-\mu^2)/E)^{-2/5}V_e^{6/5} & k>1\end{cases} \tag{26}$$

$$A_e=\begin{cases}(15/8)^{3/5}m^{3/5}r^{1/5}((1-\mu^2)/E)^{3/5}V_e^{6/5} & k=1\\ (1/2)^{1/5}(15/16)^{3/5}m^{2/5}r^{1/5}((1-\mu^2)/E)^{3/5}V_e^{6/5} & k>1\end{cases} \quad (27)$$

$$t_e=\begin{cases}2.94328(15/8)^{2/5}m^{2/5}r^{1/5}((1-\mu^2)/E)^{2/5}V_e^{-1/5} & k=1\\ 2.94328(1/2)^{1/5}(15/16)^{2/5}m^{2/5}r^{1/5} \times((1-\mu^2)/E)^{2/5}V_e^{-1/5} & k>1\end{cases} \quad (28)$$

The movement distance of the ball medium in the ascending zone per unit time is v_k, the number of ball media passing through this distance is $v_k/(2r)$. As the ball media make a continuous movement in the ascending zone, the frequency of the impact force is given by:

$$f_k=\omega R_k/(2r) \quad (29)$$

Therefore the impact grinding and attrition grinding performances are expressed by:

$$W_1=\sum_{k=1}^{N}W_{imk} \quad (30)$$

$$W_2=\sum_{k=1}^{N}W_{atk} \quad (31)$$

The synthesized grinding performance is expressed by:

$$W_3=C_1W_1+C_2W_2 \quad (32)$$

where $0\le C_1\le 1$, and $0\le C_2\le 1$. As impact grinding and attrition grinding inevitably occur in the tumbling ball mill, C_1 and C_2 should be determined by the material properties, the fineness of production and the shape of particles.

So the objective function is:

$$F(\bar{X})=-W_3 \quad (33)$$

3.2.2 Design variables We take the operation parameters of the tumbling ball mill, speed ratio ψ, filling ratio ϕ, and radius of ball media r as design variables. The design variables are given by

$$\bar{X}^T=[X_1, X_2, X_3]=[\psi, \phi, r] \quad (34)$$

As the calculation of grinding performance is based upon the accumulation of every layer, the filling layer, N, needs to be determined by filling ratio ϕ. When the radius of the shell R_0, and the rotation speed ω are determined, α_1 can be solved according to R_1 and ω by Eq.(3). As shown in Fig. 6, considering a small element within the ascending zone with a thickness of dR at a distance R from the mill center, we can deduce the areas occupied by the charge in the ascending zone and falling zone. They are:

$$F_1=\int_{R_N}^{R_0}(\lambda+\theta)RdR=8R_\rho^2\int_{\theta_N}^{\theta_0}\theta\sin(2\theta)d\theta$$
$$=8R_\rho^2(\theta\sin^2\theta-\theta/2+\sin(2\theta)/4)_{\theta_N}^{\theta_0} \quad (35)$$

$$F_2=\int_{R_N}^{R_0}4R\sin\theta\cos\theta dR$$
$$=16R_\rho^2\int_{\theta_N}^{\theta_0}\sin^2\theta\cos^2\theta d\theta$$

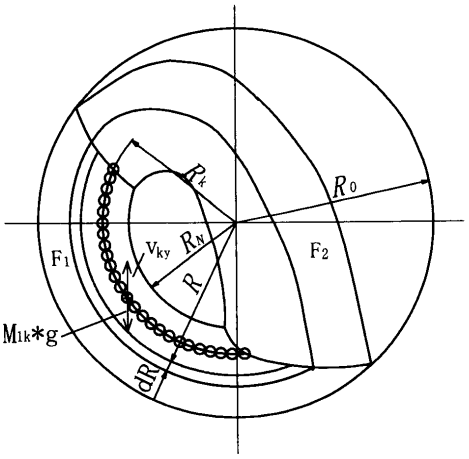

Fig. 6 Charge analysis of tumbling ball mill

$$=R_\rho^2(2\theta-\sin(2\theta)\cos(2\theta))_{\theta_N}^{\theta_0} \quad (36)$$

As the filling ratio is defined as $\phi=(F_1+F_2)/(\pi R_0^2)$, substituting Eqs.(35) and (36) into it leads to:

$$[8\theta\sin^2\theta-2\theta+\sin 2\theta(2-\cos 2\theta)]_{\theta_N}^{\theta_1}$$
$$=4\pi\phi\sin^2\theta_1 \quad (37)$$

So α_N can be solved according to the above equation by a numerical method. The area in the ascending zone occupied by a layer of media is $\Delta F_1=2rR_k(\theta_k+\lambda_k)=8rR_k\theta_k$, therefore the area in the ascending zone occupied by all layers is given by:

$$F_1=\sum_{k=1}^{N}8R_kr\theta_k \quad (38)$$

Substituting Eq.(35) into Eq.(38), the resultant equation includes two unknown variables, N and ϕ. When one variable is determined, the other one is solved accordingly.

3.2.3 Constraint functions

(1) The limitation of power of the driving motor

The opposite moment caused by the charge in the ascending zone is overcome by the driving torque of the motor. Considering the porosity of the ore and the ball media ε_g, ε_m, and the filling ratio of the ore ϕ_g, we obtain the mass of the charge:

$$M_1=(1+\phi_g\varepsilon_m(1-\varepsilon_g)\rho_g/((1-\varepsilon_m)\rho))M_m \quad (39)$$

As shown in Fig. 6, considering the ascending zone within a thickness of $2r$ at a distance R_k from the mill center, the power required to elevate the ball media and the ore in the k layer is $N_{mk}=M_{1k}gv_{ky}$. Rearranging and substituting Eqs.(4) and (39) into it, and considering the efficiency of the transmission system and overload coefficient of the motor, we obtain the power determined by the accumulation of the separation layer:

$$N_m=\sum_{k=1}^{N}(4\pi/3)r\rho R_k^2\theta_kL\phi_1g\omega\sin(2\theta_k) \quad (40)$$

where $\phi_1=1+\phi_g\varepsilon_m(1-\varepsilon_g)\rho_g/((1-\varepsilon_m)\rho)$. So the constraint is expressed by:

$$g_1(\bar{X})=N_m-N_{\text{motor}}\le 0 \quad (41)$$

Table 1 The calculation results of original and optimum design

	ϕ	ψ	r (m)	E_{max}(J)	W
Original parameters	0.42	0.76	0.04	61	3.4438
Optimized parameters	0.57	0.871	0.03	31	4.1912

(2) Constraint of the radius of inner layer media

In order to avoid the motion interference of the media, and to guarantee the falling motion and ascending motion of every layer, we require the falling points to be at or below limited positions. That is, the X-coordinate of the trajectory of the falling points must be above the minimum value. From Eq.(5), we obtain the X-coordinate of the falling point of the inner layer by rendering $k=N$:

$$X=4R_N \sin \alpha_N \cos^2 \alpha_N - R_N \sin \alpha_N \quad (42)$$

Rearranging Eq.(3) leads to $R_N=g \cos \alpha_N/\omega^2$. Substituting this into Eq.(42) and differentiating it with respect to α_N, we obtain:

$$dX/d\alpha_N=(16 \cos^4 \alpha_N-14 \cos^2 \alpha_N+1)g/\omega^2 \quad (43)$$

Letting $dX/d\alpha_N=0$, the limitations for the leaving angle of the inner layer, α_N, and the radius of the inner layer, R_N, are obtained. The radius of the inner layer should not exceed the limitation. This constraint is given by:

$$g_2(\bar{X})=g \cos \alpha_N/\omega^2-(R_0-2rN) \leq 0 \quad (44)$$

(3) The constraint of allowable maximum energy

The maximum energy of an individual ball medium is the design basis of the shell, the liners, and the bolts linking the shell and the liners. It also primarily determines the wear of the liners and the ball media. So the maximum energy of an individual ball medium would be under a certain threshold, which means that this constraint is given by:

$$g_3(\bar{X})=4\pi r^3 \rho v_{pk}^2/6-E_{\max} \leq 0 \quad (45)$$

(4) Boundary constraints

$$g_4(\bar{X})=\phi_{\min}-\phi \leq 0 \quad (46)$$

$$g_5(\bar{X})=\phi-\phi_{\max} \leq 0 \quad (47)$$

$$g_6(\bar{X})=\phi_{\min}-\phi \leq 0 \quad (48)$$

$$g_7(\bar{X})=\phi-\phi_{\max} \leq 0 \quad (49)$$

$$g_8(\bar{X})=r_{\min}-r \leq 0 \quad (50)$$

$$g_9(\bar{X})=r-r_{\max} \leq 0 \quad (51)$$

3.4 Implementation of the optimum design

The optimization of grinding performance for a tumbling ball mill is performed using the optimal algorithm of the improved constraining varied-scale method[15] (ICVM). The ICVM changes the constraint optimal problem into a series of quadratic planning sub-problems, and considers the solution of the sub-problem as the direction of the linearity searching. Meanwhile, when constituting the quadratic planning sub-problem, the ICVM uses the approximate matrix of the inverse Hessian matrix as the recurrence formula. The program for optimum design is made up of multi-modules. The modules are integrated by calling and transferring data. The structure of the program is shown in Fig. 7.

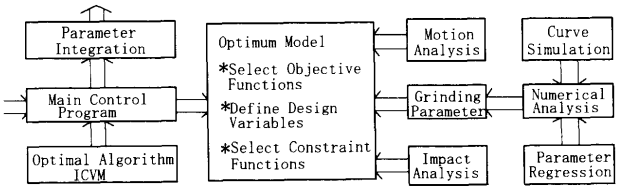

Fig. 7 Structure of the program

4. Design Results and Conclusion

According to the above analysis and mathematical model, the grinding performance of some tumbling ball mills have been optimized. The tumbling ball mill of $\Phi 3.0 \times 4$ m uses smooth liners, and is equipped with a power of 375 kW. The Young's modulus and Poisson's ratio of the ball media and liners are $E=210$ Gpa and $\mu=0.3$, respectively. The filling ratio of the ore is $\phi_g=1$. The porosities of the ball media and the ore are $\varepsilon_m=\varepsilon_g=0.4$. The average densities of the ball media and the ore are $\rho=7\,860$ kg/m^3 and $\rho_g=3\,000$ kg/m^3, respectively. The optimized parameters and the original parameters are shown in Table 1. It can be seen that the grinding performance has been increased 21.7% after the optimization. Through optimization, the range for the selection of the operation parameters is extended. For the example given above, the operation speed can reach 87% of the critical speed, instead of the conventional speed range of 70 - 78%, and the filling ratio of the ball media can reach 57%, instead of the conventional filling ratio of 40 - 50%. Meanwhile the maximum energy of the individual ball medium falls from 61 J to 31 J, which is advantageous in terms of the strength of the mill and wear of the media and the liners.

The above results agree in part with the experimental results of other researchers. For example, Mishra and Rajamani[3),(4)] obtained a frequency distribution of impact energy for $\psi=60\%$ and $\psi=80\%$. The total energy of the latter is much greater than that of the former. Moys et al.[16] measured the forces exerted by the ball media on the liners in a ball mill at several different speed ratios, which showed that at $\psi=77\%$ and $\psi=86\%$, the forces exerted on the liners rose more rapidly.

This research provides an approach for the optimi-

zation of grinding performance for tumbling ball mills. The equations of motion, impact parameters and grindability have been established, and used as the objective and constraints functions for the optimization of grinding performance. The grinding performance under the optimized operation parameters is improved significantly.

Substantial further work is required to validate these predictions and to improve the mathematical model for multi-points stacking and impacting.

References

(1) Bond, F.C., Grinding Ball Size Selection, Mining Eng., Vol. 10 (1958), pp. 592-595.

(2) Viswanathan, K. and Mani, B.P., Optimum Method of Calculation of Product Distribution from a Distributed Fracture Model, International Journal of Mineral Processing, Vol. 11, No. 2 (1983), pp. 155-162.

(3) Mishra, B.K. and Rajamani, R.K., Simulation of Charge Motion in Ball Mills—Part 1: Experimental Verifications, International Journal of Mineral Processing, Vol. 40, No. 4 (1994), pp. 171-186.

(4) Mishra, B.K. and Rajamani, R.K., Simulation of Charge Motion in Ball Mills—Part 2: Numerical Simulations, International Journal of Mineral Processing, Vol. 40, No. 4 (1994), pp. 187-197.

(5) Powell, M.S. and Nurick, G.N., A Study of Charge Motion in Rotary Mills—Part 1: Extension of the Theory, Minerals Engineering, Vol. 9, No. 2 (1996), pp. 259-268.

(6) Powell, M.S. and Nurick, G.N., A Study of Charge Motion in Rotary Mills—Part 2: Experimental Work, Minerals Engineering, Vol. 9, No. 3 (1996), pp. 343-350.

(7) Powell, M.S. and Nurick, G.N., A Study of Charge Motion in Rotary Mills—Part 3: Analysis of Results, Minerals Engineering, Vol. 9, No. 4 (1996), pp. 399-418.

(8) Yashima, S., Kanda, Y. and Sano, S., Relationships Between Particle Size and Fracture Energy or Impact Velocity Required to Fracture as Estimated from Single Particle Crushing, Powder Technology, Vol. 51, No. 3 (1987), pp. 277-282.

(9) Grady, D.E. and Kipp, E., Fracture Mechanics of Rock, (1987), Academic Press.

(10) Andrews, E.W. and Kim, K.S., Threshold Conditions for Dynamics Fragmentation of Ceramic Particles, Mechanics of Materials, Vol. 29, No. 3 (1998), pp. 161-180.

(11) Prasher, C.C., Crushing and Grinding Process Handbook, (1987), John Wiley and Sons Limited.

(12) Brach, R.M., Impact Coefficients and Tangential Impacts. Transactions of the ASME, Journal of Applied Mechanics, Vol. 64, No. 4 (1997), pp. 1014-1016.

(13) Hutchings, I.M., Strain Rate Effects in Microparticle Impact, Journal of Physics D: Applied Physics, Vol. 10, No. 2 (1975), pp. L179-L184.

(14) Thornton, C., Coefficient of Restitution for Collinear Collisions of Elastic-Perfectly Plastic Spheres, Transaction of the ASME: Journal of Applied Mechanics, Vol. 64, No. 2 (1997), pp. 383-386.

(15) Vanderplaats, G.I.N., Numeral Optimization Techniques for Engineering Design with Application, (1984), McGraw-Hill.

(16) Moys, M.H., Smit, I. and Stange, W., The Measurement of Forces Exerted by the Load on Liners in Rotary Mills, International Journal of Mineral Processing, Vol. 44-45, No. 4 (1996), pp. 383-393.